Reprinted from September 1976, Vol. 98, Journal of Dynamic Systems, Measurement, and Control

A Nonlinear Dynamic Model of a Once-Through Subcritical Steam Generator

A. RAY[1]

Control Engineer,
Stone & Webster Engineering Corp.,
Boston, Mass.

H. F. BOWMAN

Associate Professor,
Department of Mechanical Engineering,
Northeastern University,
Boston, Mass.
Assoc. Mem. ASME

A dynamic thermal-hydraulic model of a once-through subcritical steam generator is presented which allows the investigation of power plant system transients. The three-section (economizer, evaporator, and superheater) model with time-varying phase boundaries is described by a set of nonlinear differential and algebraic equations derived from the fundamental equations of conservation of mass, momentum, and energy. The transient response of 8 process variables, due to 5 percent independent step disturbances in 5 input variables at 100 percent load, is discussed.

Introduction

The thermal-hydraulic transients of the steam generator are essential in the study of the overall system performance of both nuclear and fossil-fueled power plants as well as for the design of their appropriate control systems. These transients are described here by a nonlinear dynamic model of the steam generator. For efficient digital simulation of the overall system, the steam generator model should be optimized for computation cost and accuracy. Fine mesh models [1, 2][2] give good representation of the system dynamics at the cost of increased model complexity and require a relatively small iteration time step for numerical stability and convergence of the solution. To circumvent this problem, a nonlinear dynamic model of the once-through subcritical steam generator [3] was formulated using the concept of time-varying phase boundaries. This concept was first introduced by Adams et al. [4], for analog simulation of a linearized model of such a steam generator.

The basic model equations were derived form the integral forms of the fundamental equations of conservation of mass, momentum, and energy [5, 6] through the control volume approach. The numerical results for the transient response of selected system variables were obtained by simulating the set of nonlinear differential and algebraic equations on an IBM 370 computer using Continuous System Modeling Program (CSMP III) [7].

The method of analysis and study of numerical stability and frequency range of this model will be presented in a future publication.

System Description

The once-through subcritical steam generator considered in this analysis is typical of those used in gas-cooled nuclear power plants. It consists of a large number of helically coiled tubes of vertical orientation. Each tube was treated as a counterflow heat exchanger. Hot gas (primary coolant) is circulated through the shell of the steam generator from the top, and compressed water (secondary coolant) is pumped through the steam generator tubes from the bottom. Thermal energy from the primary coolant (gas) is transferred to the secondary coolant (water/steam) through the tube walls. The exchange of thermal energy results in the cooling of the hot gas on the shell side of steam generator and production of superheated steam on the tube side.

The model was based on the performance of a typical tube shown schematically in Fig. 1(*a*).

Assumptions

The fundamental assumption of this study was that the distributed parameter process can be represented by a lumped parameter model using the concept of control volumes. In addition, the following assumptions were made:

(*a*) Uniform fluid properties over any cross-section.
(*b*) Uniform and independent heat fluxes across the tube wall for each section.
(*c*) Identical flow through each of the steam generator tubes.
(*d*) Steady primary coolant flow.
(*e*) Constant primary coolant pressure.
(*f*) Primary coolant treated as a perfect gas.

Further, the following parameters were evaluated and were

[1]Now with the MITRE Corporation, Bedford, Mass.

[2]Numbers in brackets designate References at end of paper.

Contributed by the Automatic Control Division for publication in the JOURNAL OF DYNAMIC SYSTEMS, MEASUREMENT, AND CONTROL. Manuscript received at ASME Headquarters, October 24, 1975. Paper No. 76-Aut-M.

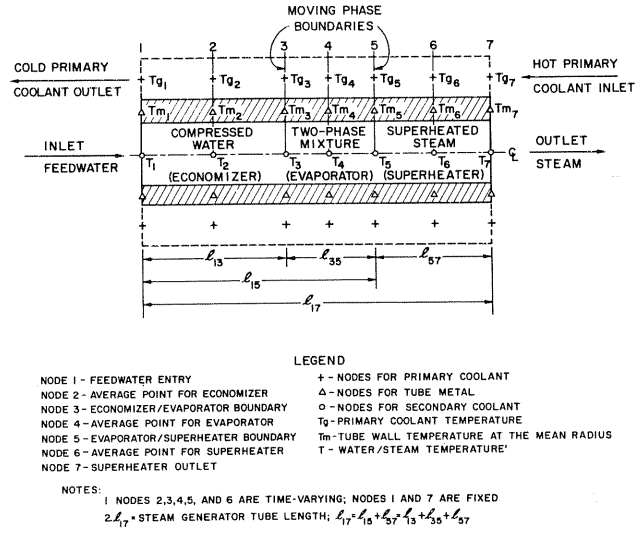

Fig. 1(*a*) Schematic view of a single tube of steam generator with time-varying phase boundaries

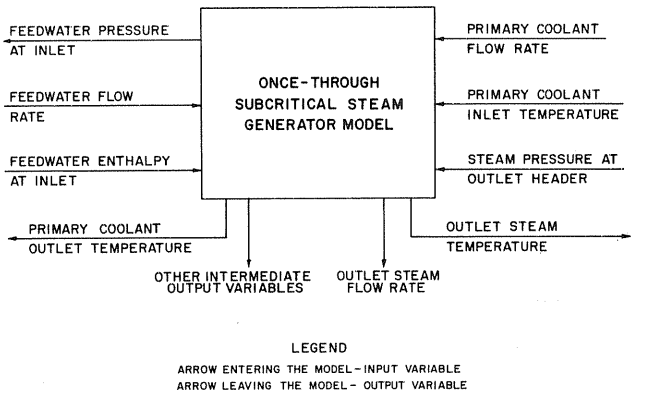

Fig. 1(*b*) Steam generator model solution diagram

found to be negligible:

(*a*) Axial conduction of heat in primary coolant, tube wall, and secondary coolant.
(*b*) Velocity head of water/steam in each section.
(*c*) Thermal radiation from primary coolant to tube wall.

Development of Model Equations

A typical tube of the once-through subcritical steam generator was partitioned into three sections, i.e., compressed water (economizer), wet steam (evaporator), and superheated steam (superheater), as shown in Fig. 1(*a*). The length of each section was allowed to vary with time. Thus, the other process variables such as pressure, temperature, flow, etc, at these phase boundaries were also time-varying.

The model equations were devloped using control volumes with time-varying control surfaces as shown in Fig. 1(*a*). A model solution diagram indicating the input and output variables is given as Fig. 1(*b*). The model equations for secondary coolant, primary coolant, and tube wall are discussed below:

Secondary Coolant. Variations in thermodynamic properties of the secondary coolant in different phases and the effect of relative velocity with respect to the moving phase boundaries required the formulation of model equations in unique ways.

The continuity equations for the secondary coolant in each of the three regions are as follows:

Economizer

$$d(\rho_2 l_{13})/dt = (W_1 - W_3)/A + \rho_3 dl_{13}/dt \quad (1)$$

Evaporator

$$d(\rho_4 l_{35})/dt = (W_3 - W_5)/A - \rho_3 dl_{13}/dt + \rho_5 dl_{15}/dt \quad (2)$$

Superheater

$$d(\rho_6 l_{57})/dt = (W_5 - W_7)/A - \rho_5 dl_{15}/dt \quad (3)$$

where

$$\frac{dl_{15}}{dt} = \frac{dl_{13}}{dt} + \frac{dl_{35}}{dt} = -\frac{dl_{57}}{dt}$$

Energy equations for the secondary coolant follow for each of the three regions:

Economizer

$$d(\rho_2 u_2 l_{13})/dt = (W_1 h_1 - W_3 h_3 + Q_2)/A + \rho_3 h_3 dl_{13}/dt \quad (4)$$

Evaporator

$$d(\rho_4 u_4 l_{35})/dt = (W_3 h_3 - W_5 h_5 + Q_4)/A - \rho_3 h_3 dl_{13}/dt + \rho_5 h_5 dl_{15}/dt \quad (5)$$

Nomenclature

A = tube cross-sectional area for secondary coolant flow
A_i = inner circumference of tube
A_g = unit cross-sectional area for primary coolant flow
A_0 = outer circumference of tube
C_m = thermal capacity of tube per unit length
C_p = specific heat of primary coolant
C_v = specific heat of primary coolant
G = primary coolant flow rate per tube
g = local acceleration due to gravity
h = specific enthalpy of secondary coolant
K_f = fluid pressure drop constant
K_{gm} = heat transfer coefficient constants for primary coolant
K_{mf} = heat transfer coefficient constants for secondary coolant
$K_{\rho T}$ = product of absolute temperature and density of primary coolant
k_m = thermal conductivity of tube metal
l = length of tube or tube section
P = secondary coolant pressure
Q_g = heat transfer rate from primary coolant to tube wall
Q = heat transfer rate from tube wall to secondary coolant
r_i = inside tube radius
r_0 = outside tube radius
r_m = mean tube radius
T = secondary coolant temperature
T_g = primary coolant temperature
T_m = tube wall temperature at mean radius
t = time
U = heat transfer coefficient
u = specific internal energy of secondary coolant
W = secondary coolant mass flow rate per tube with respect to tube wall
x = quality factor
τ_d = delay time
ρ = density of secondary coolant
ρ_g = density of primary coolant
θ = average horizontal inclination of helically coiled tubes

Superheater

$$d(\rho_6 u_6 l_{57})/dt = (W_5 h_5 - W_7 h_7 + Q_6)/A - \rho_5 h_5 dl_{15}/dt \quad (6)$$

For the economizer, combination of equations (1) and (4) yields equations (7) and (8):

$$dl_{13}/dt = \left[W_1 - W_3 - \left(\frac{\partial \rho_2}{\partial u_2} \right)_{P2} (W_1(h_1 - u_2) - W_3(h_3 - u_2) + Q_2)/\rho_2 \right] \Big/ \left[A \left((\rho_2 - \rho_3) + (\rho_3/\rho_2) \left(\frac{\partial \rho_2}{\partial u_2} \right)_{P2} (h_3 - u_2) \right) \right] \quad (7)$$

where

$$d\rho_2 = \left(\frac{\partial \rho_2}{\partial u_2} \right)_{P2} du_2 + \left(\frac{\partial \rho_2}{\partial P_2} \right)_{u2} dP_2 \approx \left(\frac{\partial \rho_2}{\partial u_2} \right)_{P2} du_2$$

for compressed water in the range of pressure of interest, and

$$du_2/dt = [(W_1(h_1 - u_2) - W_3(h_3 - u_2) + Q_2)/A + \rho_3(h_3 - u_2)dl_{13}/dt]/(\rho_2 l_{13}) \quad (8)$$

For the evaporator, equations (2) and (5) yield

$$dl_{15}/dt = [\rho_3(h_3 - u_4)dl_{13}/dt - (W_3(h_3 - u_4) - W_5(h_5 - u_4) + Q_4)/A + \rho_4 l_{35} du_4/dt]/(\rho_5(h_5 - u_4)) \quad (9)$$

In the pressure range of interest (i.e., close to the critical pressure), the thermodynamic properties of water/steam mixture reveal that the partial derivative of specific internal energy with respect to pressure changes sign monotonically between 0 and 100 percent quality. Thus, u_4 was not chosen as a state variable as it cannot be analytically formulated to represent the lumped characteristics of the evaporator. Consequently, l_{15} was chosen as a state variable and du_4/dt was computed as a weighted average of the derivatives of fluid properties at the evaporator exit boundary and economizer average point.

For the superheater, equations (3) and (6) yield

$$du_6/dt = [(W_5(h_5 - u_6) - W_7(h_7 - u_6) + Q_6)/A - \rho_5(h_5 - u_6)dl_{15}/dt]/(\rho_6 l_{57}) \quad (10)$$

In order to increase the size of the time step for numerical integration, the continuity equations for the evaporator and the superheater were combined together as,

$$\frac{d}{dt}[\rho_5(l_{35} + l_{57})] = (W_3 - W_7)/A - \rho_3 dl_{13}/dt$$

which yields

$$d\rho_5/dt = [(W_3 - W_7)/A + (\rho_5 - \rho_3)dl_{13}/dt]/(l_{35} + l_{57}) \quad (11)$$

A study of the temporal acceleration term in the momentum equations revealed very fast decaying transients due to low inertia of the steam/water path. The control system and the process external to the steam generator behave as low pass filters with respect to these fast transients. Hence, these transients have little bearing on the design of control systems. Further, the time step size of integration used in this analysis is large in comparison to the period of these transients. Thus, the temporal acceleration terms have been omitted in the momentum equations as stated below:

Economizer

$$P_1 = P_3 + K_{f2} W_1^2 l_{13}/\rho_2 + \rho_2 g l_{13} \sin\theta \quad (12)$$

where the spatial average feedwater flow W_2 was taken to be equal to the inlet feedwater flow W_1, as the coolant is incompressible in this region.

Evaporator

$$W_3 = \sqrt{(P_3 - P_5 - \rho_4 g l_{35} \sin\theta)\rho_4/(K_{f4} l_{35})} \quad (13)$$

where the average coolant flow W_4 through the evaporator was set equal to the inlet flow W_3 in the evaporator.

Superheater

$$W_7 = \sqrt{(P_5 - P_7 - \rho_6 g l_{57} \sin\theta)\rho_6/(K_{f6} l_{57})} \quad (14)$$

where the superheated steam flow W_7 out of the steam generator was taken to be equal to the spatial average flow W_6 in the superheater.

The saturated steam flow W_5 at the evaporator/superheater boundary was computed as an arithmetic average of W_3 and W_7.

Transport Delay. Any change in enthalpy at the inlet of a control volume is not immediately sensed at the outlet of that control volume particularly in the case of economizer where the velocity of flow and mixing of feedwater are relatively small. The outlet enthalpy (saturated water) in this analysis was based on an extrapolation of inlet and spatial average enthalpies. Thus, to accurately represent the process, a transport delay term $\tau_d = A l_{13} \rho_2 / W_1$ was necessary.

The effect of transport delay was approximated by a first order lag equal to about half the transport delay. Operational changes in inlet enthalpy occur slowly (because of large thermal inertia of deaerator) and thus the above equation rather closely approximates the actual operating conditions.

Heat Transfer. Heat transfer from the primary coolant to the tube wall and from the tube wall to the secondary coolant was assumed to be due entirely to convection. Radial heat transfer through the tube wall was due to conduction. The temperature nodes in the tube wall were taken at the mean radius.

Convective heat transfer for fully developed single phase turbulent flow was computed by Dittus and Boelter equation [8, 9]. Since the thermal and hydraulic property changes of the primary coolant, compressed water, and superheated system are insignificant in comparison to the changes in fluid velocity, the heat transfer coefficient for a single phase fully developed turbulent flow was expressed as, $U = W^n/K_u$, where W is mass flow rate of fluid and K_u and n are constants.

For a fully developed two phase flow, the heat transfer is primarily due to nucleate boiling in the low quality factor region and to partial film boiling in the high quality factor region [10]. For nucleate boiling, the heat transfer coefficient has been given by Levy [10] and was approximated as $U \propto P^{4/3}(\Delta T)^2$. The heat transfer coefficient for the partial film boiling regime was obtained by using the data [10] given by Bertoletti, et al. The average heat transfer coefficient between the tube wall and the two phase coolant was obtained by graphically integrating the local heat transfer coefficient over the entire length of the evaporator.

The rates of heat transfer [8] due to turbulent flow of the primary coolant over the tube walls in the three regions were computed as Economizer

$$Q_{g2} = A_0 l_{13}(T_{g2} - T_{m2})/[K_{gm2} G^{-0.66} + C_0] \quad (15)$$

where

$$C_0 = [r_0 \ln(r_0/r_m)]/k_m \text{ and } r_m = (r_0 + r_i)/2$$

Evaporator

$$Q_{g4} = A_0 l_{35}(T_{g4} - T_{m4})/[K_{gm4} G^{-0.66} + C_0] \quad (16)$$

Superheater

$$Q_{g6} = A_0 l_{57}(T_{g6} - T_{m6})/[K_{gm6} G^{-0.66} + C_0] \quad (17)$$

The rates of heat transfer between the tube wall and the secondary coolant for the three regions were calculated as

Economizer

$$Q_2 = A_i l_{13}(T_{m2} - T_2)/[K_{mf2}W_1^{-0.8} + C_i] \quad (18)$$

where

$$C_i = [r_i \ln (r_m/r_i)]/k_m$$

Evaporator

$$Q_4 = A_i l_{35}(T_{m4} - T_4)/[K_{mf4} + C_i] \quad (19)$$

Superheater

$$Q_6 = A_i l_{57}(T_{m6} - T_6)/[K_{mf6}W_7^{-0.8} + C_i] \quad (20)$$

Energy Equation in Tube Wall. The tube wall temperatures T_{m3} and T_{m5} at the economizer/evaporator and the evaporator/superheater boundaries, respectively, were expressed in terms of the average temperatures T_{m2}, T_{m4}, and T_{m6} as

$$T_{m3} = (l_{35}T_{m2} + l_{13}T_{m4})/l_{15} \quad (21)$$

$$T_{m5} = (l_{57}T_{m4} + l_{35}T_{m6})/(l_{35} + l_{57}) \quad (22)$$

For the three regions of time-varying dimensions, the dynamic equations for energy storage in the tube wall were formulated from the energy balance in the tube wall as shown:

Economizer

$$\frac{dT_{m2}}{dt} = (Q_{g2} - Q_2)/(C_m l_{13}) + ((T_{m4} - T_{m2})/l_{15})dl_{13}/dt \quad (23)$$

Evaporator

$$\frac{dT_{m4}}{dt} = (Q_{g4} - Q_4)/(C_m l_{35}) + ((T_{m6} - T_{m4})/(l_{35} + l_{57}))dl_{15}/dt + ((T_{m4} - T_{m2})/l_{15})dl_{13}/dt \quad (24)$$

Superheater

$$\frac{dT_{m6}}{dt} = (Q_{g6} - Q_6)/(C_m l_{57}) + ((T_{m6} - T_{m4})/(l_{35} + l_{57}))dl_{15}/dt \quad (25)$$

Primary Coolant. The dynamic terms in the continuity equations were not considered because the fluid at low linear velocity was treated as incompressible. Further, the pressure drops due to acceleration and friction were neglected since they are insignificant in comparison to the absolute pressure of the primary coolant.

In the superheater, the energy equation for the primary coolant can be expressed as

$$(A_g C_v K_{\rho T})dl_{57}/dt = G(T_{g7} - T_{g5})C_p + A_g C_p K_{\rho T} dl_{15}/dt - Q_{g6} \quad (26)$$

For a linear temperature profile along the length of steam generator tube, the average temperatures T_{g6}, T_{g4}, and T_{g2} of the primary coolant were computed as arithmetic means of the end point temperatures for each of the three regions.

Combining equations (17) and (26), and using the relation $T_{g6} = (T_{g7} + T_{g5})/2$ yields

$$T_{g5} = [T_{g7}(1 - Y_6) + 2Y_6 T_{m6} - Y_g dl_{15}/dt]/(1 + Y_6) \quad (27)$$

where

$$Y_6 = A_0 l_{57}/[2(K_{gm6}G^{-0.66} + C_0)GC_p],$$

and

$$Y_g = (C_p - C_v)A_g K_{\rho T}/(GC_p) \text{ and } C_0 = [r_0 \ln (r_0/r_m)]/k_m.$$

Similarly, the energy equations for the primary coolant in the evaporator and economizer regions yield

$$T_{g3} = [T_{g5}(1 - Y_4) + 2Y_4 T_{m4} + Y_g dl_{35}/dt]/(1 + Y_4) \quad (28)$$

$$T_{g1} = [T_{g3}(1 - Y_2) + 2Y_2 T_{m2} + Y_g dl_{13}/dt]/(1 + Y_2) \quad (29)$$

where

$$Y_4 = A_0 l_{35}/[2(K_{gm4}G^{-0.66} + C_0)GC_p]$$

and

$$Y_2 = A_0 l_{13}/[2(K_{gm2}G^{-0.66} + C_0)GC_p]$$

A summary of the equation set which constitutes the model is listed in the Appendix.

System Parameters. The system parameters were calculated from the end point values of the process variables (e.g., pressure, temperature, length, etc.) for each region at the rated conditions, and the physical dimensions of the steam generator tube. These data and the steady state model results are listed in Table 1. The steady state values of average tube wall temperature were determined from energy balance data. Knowing the friction factors and steady state pressure drop, the steady state values of spatial average density for the secondary coolant were calculated for each region. For two phase flow in the evaporator, the Martinelli-Nelson correction factor [8] was applied.

From the knowledge of temperature and density at the average points, the other properties were determined via the thermodynamic state relations. The averaging constants were then calculated from the steady-state values of individual variables at the inlet, outlet, and average points.

Results and Discussion

The steady state performance of the nonlinear dynamic model was tested at the 100 percent and 50 percent rated conditions, respectively. Table 1 shows that the model results agree favorably with the heat balance data.

The results of the steam generator system simulation are presented in the form of a series of curves representing the transient response of the process variables at the rated conditions for independent step increases in 5 different input variables. In each case, the input variable under study was perturbed from its operating point by a 5 percent step increase with the other 4 input variables held constant. The following 5 input variables (Fig. 1(*b*)) were perturbed:

1 Primary coolant flow rate
2 Primary coolant inlet temperature
3 Steam pressure at superheater outlet
4 Inlet feedwater flow rate
5 Inlet feedwater enthalpy

Five curves, each showing the transient response of a given process variable to a change in one of the 5 input variables, are displayed in a single figure. Fig. 2–9 show the transient response of 8 different output variables for changes in each of the 5 input variables listed above.

Run No. 1 shows the system transient response for a 5 percent step increase in primary coolant flow rate with the other 4 input variables held constant. Increased primary coolant flow rate increases the rate of heat transfer from the primary coolant to the secondary coolant through the tube wall. The lengths of economizer and evaporator (Figs. 2 and 3) decrease, whereas the length of superheater (Fig. 4) increases. For constant outlet steam header pressure and feedwater flow rate, the inlet feedwater pressure (Fig. 6) increases, due to a larger pressure drop across the steam generator tube (the largest pressure drop occurs across the superheater). The temperature of steam leaving the steam generator (Fig. 5), after a small initial dip, steadily increases to a new steady state value. The enthalpy of saturated water at the economizer/evaporator boundary (Fig. 7) increases and the enthalpy of saturated steam at the evaporator/super-

Table 1 Physical dimensions, heat balance data, and steady state model performance

Dimensions of a Typical Steam Generator Tube

length	349 ft 106.375 m	I. D.	0.06083 ft 0.01854 m	O. D.	0.08333 ft 0.02534 m

Process variables		Rated steam flow rate		50% Rated steam flow rate		Remarks
		Heat balance data	Model results	Heat balance data	Model results	
G	lb/sec	2.19	2.19	1.235	1.235	Model
	kg/sec	0.9934	0.9934	0.5602	0.5602	Input
h_1	Btu/lbm	347.0	347.0	293.4	293.4	Model
	W-sec/kg	0.80693e + 06	0.80693e + 06	0.68228e + 06	0.68228e + 06	Input
h_7	Btu/lbm	1422.5	1422.6	1422.5	1424.2	
	W-sec/kg	3.30793e + 06	3.30813e + 06	3.30793e + 06	3.3119e + 06	
l_{13}	ft	176.0	175.94	172.0	173.7	
	m	53.645	53.627	52.426	52.944	
l_{35}	ft	82.0	81.78	90.0	90.38	
	m	24.994	24.927	27.432	27.548	
l_{57}	ft	91.0	91.28	87.0	84.92	
	m	27.737	27.822	26.518	25.884	
P_1	psia	2848.0	2847.5	2536.0	2533.8	
	N/m²	288.57e + 06	288.52e + 06	256.96e + 06	256.74e + 06	
P_3	psia	2818.0	2817.3	2524.0	2521.7	
	N/m²	285.53e + 06	285.46e + 06	255.74e + 06	255.51e + 06	
P_5	psia	2744.0	2743.6	2500.0	2498.3	
	N/m²	278.03e + 06	278.00e + 06	253.31e + 06	253.14e + 06	
P_7	psia	2600.0	2600.0	2462.0	2462.0	Model
	N/m²	253.45e + 06	253.45e + 06	249.46e + 06	249.46e + 06	Input
T_{g1}	°F	623.6	623.64	562.6	561.68	
	°C	328.67	328.69	294.78	294.27	
T_{g7}	°F	1247.3	1247.3	1140.4	1140.4	Model
	°C	675.17	675.17	615.78	615.78	Input
W_1	lbm/sec	1.577	1.577	0.785	0.785	Model
	kg/sec	0.7153	0.7153	0.3561	0.3561	Input

heater boundary (Fig. 8) decreases due to increases in pressure at each boundary. The different enthalpy-pressure relationships of saturated liquid and vapor near the critical pressure are important in the analysis of the dynamic behavior of once-through subcritical steam generators. The rate of steam flow out of the steam generator (Fig. 9) initially rises and then approaches the original value as there is no increase in feedwater flow to sustain the rise. The transient response curves of the system output variables are almost monotonic and settle down in approximately 80 s. The time lag is primarily due to the thermal inertia which consists of the thermal capacitance of the metal mass in the tube wall and the thermal resistance in the heat flow path from the primary coolant ot the secondary coolant.

Run No. 2 shows the same system transient responses for a 5 percent step increase in primary coolant inlet temperature with the other 4 input variables held constant. Increased temperature of the primary coolant increases the rate of transfer of thermal energy to the secondary coolant through the tube wall. The

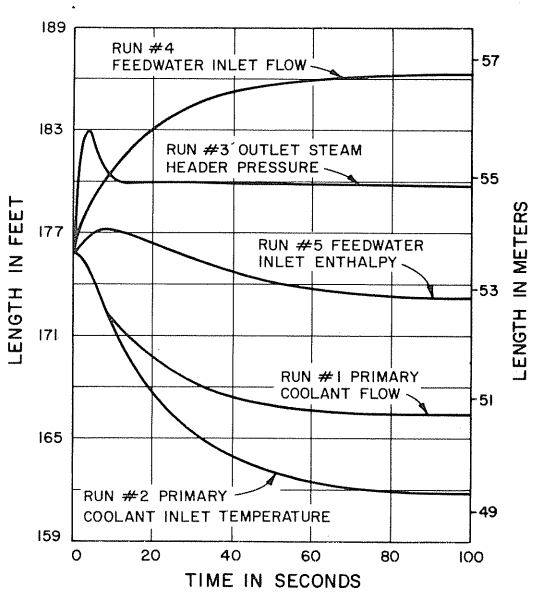

Fig. 2 Economizer length transients due to 5 percent independent step increases in 5 input variables at 100 percent load (run #'s 1-5)

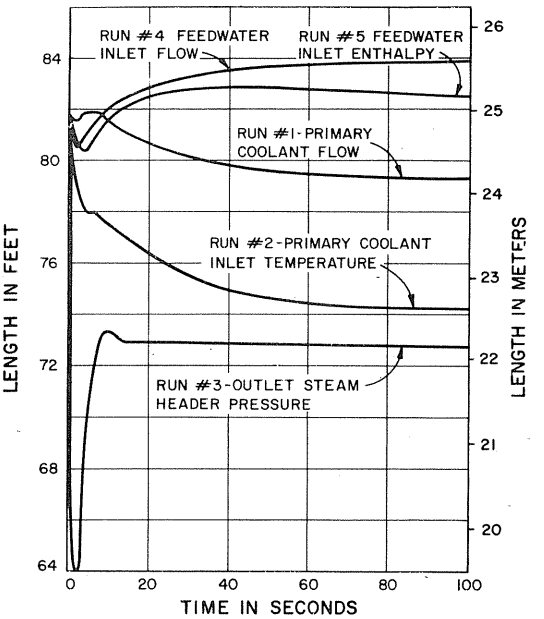

Fig. 3 Evaporator length transients due to 5 percent independent step increases in 5 input variables at 100 percent load (run #'s 1-5)

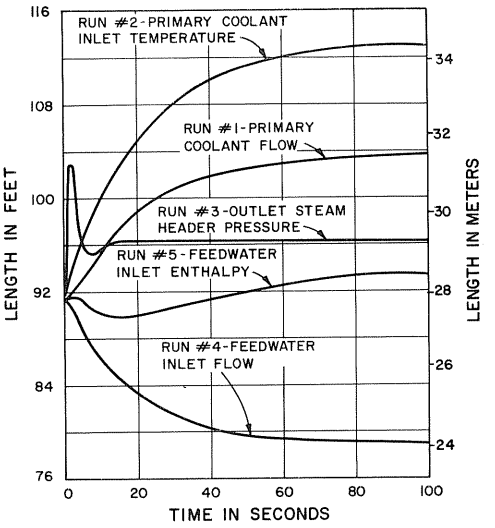

Fig. 4 Superheater length transients due to 5 percent independent step increases in 5 input variables at 100 percent load (run #'s 1-5)

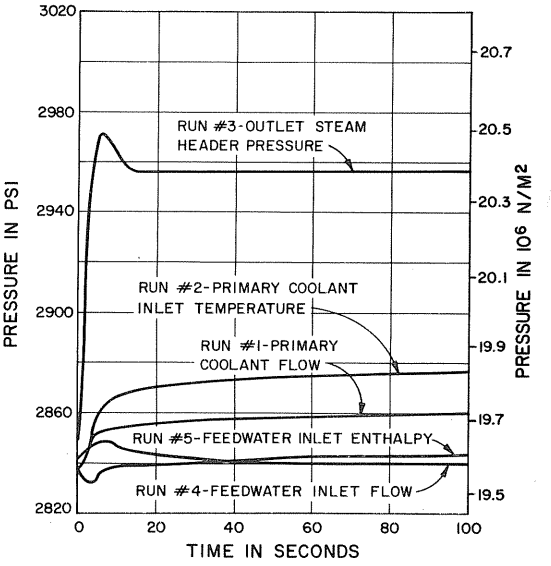

Fig. 6 Feedwater inlet pressure transients due to 5 percent independent step increases in 5 input variables at 100 percent load (run #'s 1-5)

system transient responses for this run are qualitatively similar to those of run No. 1; but the process variables are quantitatively more perturbed.

Run No. 3 shows the system transient responses for a 5 percent step increase in outlet steam header pressure with the other 4 input variables held constant. Since the feedwater flow rate is unchanged, the fluid pressure throughout the steam generator increases. Thus, the subcritical steam generator approaches a supercritical steam generator which results in a large decrease in the length of the evaporator (Fig. 3) and corresponding increases in the lengths of both economizer and superheater (Figs. 2 and 4). Significant rise in water/steam pressure throughout the steam generator tube causes a sharp increase and decrease in the enthalpies at the economizer/evaporator and evaporator/superheater boundaries (Figs. 7 and 8), respectively. The increase in downstream header pressure causes an abrupt decrease in steam flow rate out of the steam generator (Fig. 9) which quickly settles down to the original value as there is no change in the inlet feedwater flow rate. The temperature of steam leaving

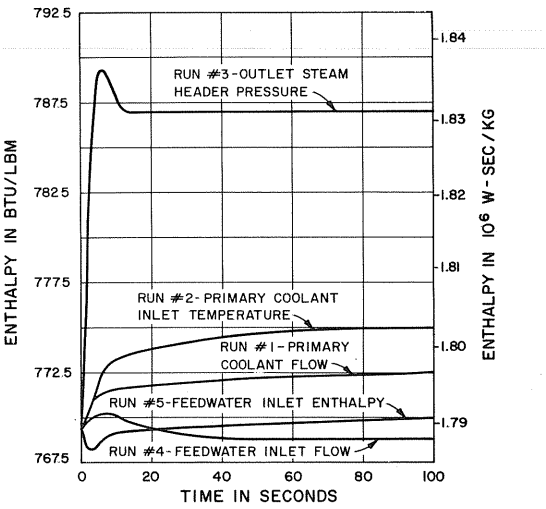

Fig. 7 Saturated water enthalpy transients due to 5 percent independent step increases in 5 input variables at 100 percent load (run #'s 1-5)

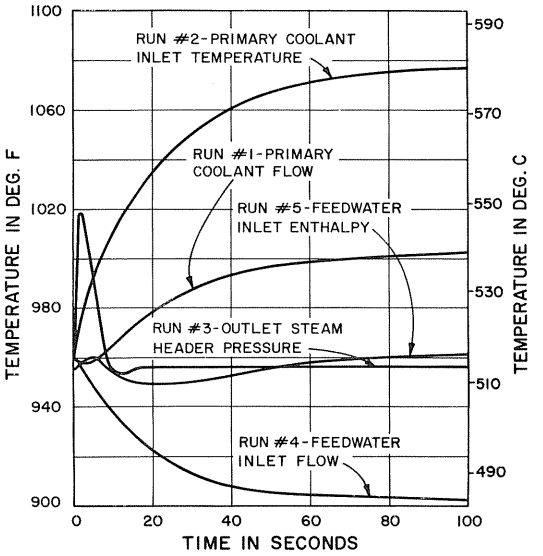

Fig. 5 Superheater outlet steam temperature transients due to 5 percent independent step increases in 5 input variables at 100 percent load (run #'s 1-5)

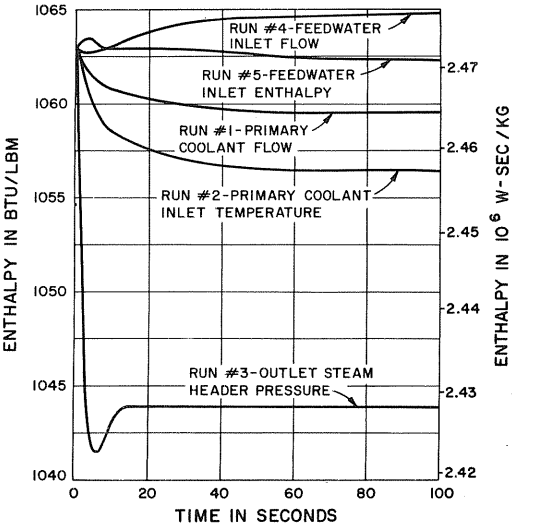

Fig. 8 Saturated steam enthalpy transients due to 5 percent independent step increases in 5 input variables at 100 percent load (run #'s 1-5)

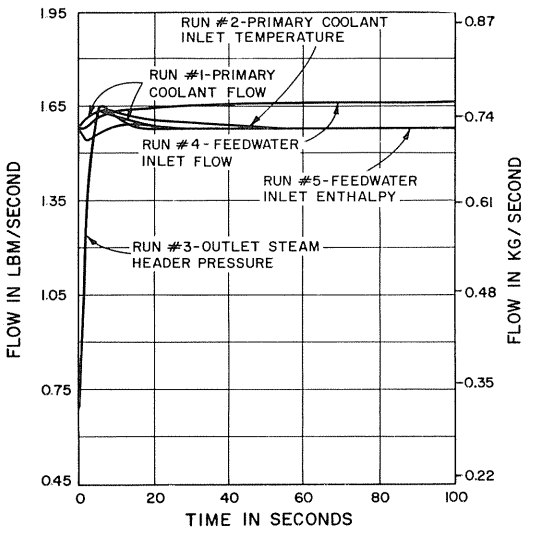

Fig. 9 Outlet steam flow transients due to 5 percent independent step increases in 5 input variables at 100 percent load (run #'s 1-5)

the steam generator (Fig. 5) increases initially due to the drop in steam flow rate and then relaxes back close to the original value as the rate of energy input to the system and the feedwater flow rate are unchanged. All the system transients for the perturbation of outlet steam header pressure completely decay within 20 s. The response times for this run are faster than those for runs. Nos. 1 and 2 because the disturbance, in this case, is hydraulic whereas those for runs Nos. 1 and 2 were thermal.

Run No. 4 shows the system responses for a 5 percent step increase in feedwater flow rate with the other 4 input variables held constant. Steam flow out of the steam generator (Fig. 9) is unresponsive to the increased feedwater flow rate for a period of approximately 2 s, and essentially equals the increased feedwater flow rate within 50 s. For constant primary coolant flow rate and inlet temperature, the temperature at all points in the secondary water/steam path drops due to the increased feedwater flow rate. Consequently, the lengths of economizer and evaporator (Figs. 2 and 3) increase and the length of superheater (Fig. 4) decreases. The inlet feedwater pressure (Fig. 6) increases initially due to a larger pressure drop across the steam generator caused by the increase in feedwater flow rate. Subsequently, the decrease in superheater length (Fig. 4) overcompensates for the increase in feedwater flow rate and the inlet feedwater pressure asymptotically approaches a value slightly lower than its initial value. The coupled hydraulic/thermal transients observed here have response times which are intermediate between the thermal transients of runs Nos. 1 and 2 and the hydraulic transients of run No. 3.

Run No. 5 shows the system transient responses for a 5 percent step increase in inlet feedwater enthalpy with the other 4 input variables held constant. Each process variable (Figs. 2–9) displays an initial reverse oscillation with a subsequent asymptotic behavior. Probably, these oscillations in the model results are generated due to extrapolation of enthalpy (h_3) of saturated water from inlet and average point enthalpies (h_1 and h_2) in the economizer. However, the long term transients of the process variables can be justified for an increased thermal energy input to the secondary coolant circuit at the economizer inlet. These transients are of the order of 60 s, reflecting the effect of thermal transport delay and thermal/hydraulic time lag.

Conclusions

A three-section dynamic model of a once-through subcritical steam generator with time-varying phase boundaries has been presented. The steam generator under consideration was of the type used in gas-cooled nuclear power plants. The system transients derived from this model are useful to the design of appropriate control systems. Further, the model can be used as an element in an overall system performance study of large scale nuclear power plants. For application to fossil-fueled power plants, the effect of radiation should be included in the calculation of heat transfer from the flames/flue gas to the tube wall.

By including the temporal acceleration terms in the momentum equations, this model could be used for microscopic flow stability studies of individual steam generator tubes.

Acknowledgments

The authors acknowledge the benefits of discussions with the first author's former colleagues Mrs. N. E. Pettengill, Dr. S. M. Joshi, and Mr. J. A. Rovnak. This paper represents part of a Mechanical Engineer Degree Thesis completed by the first author at Northeastern University in June, 1974.

References

1 Shang, T. L., "A Dynamic Model for a Once-Through Supercritical Pressure Boiler," PhD thesis, 1971, Swiss Federal Institute of Technology, Zurich.

2 Ahner, D. J., deMello, F. P., Dyer, C. E., and Sumner, V. C., "Analysis and Design of Controls for a Once-through Boiler Through Digital Simulation," *ISA Proceedings*, 9th National Power Instrumentation Symposium, May, 1966.

3 Ray, A., "A Nonlinear Dynamic Model of Once-through Subcritical Steam Generator," Mechanical Engineer Thesis, 1974, Northeastern University, Boston.

4 Adams, J., Clark, D. R., Louis, J. R., and Spanbauer, J. P., "Mathematical Modeling of Once-through Boiler Dynamics," *IEEE Trans.*, PAS-84, Feb. 1965, pp. 146–156.

5 Batchelor, G. K., *An Introduction to Fluid Dynamics*, Cambridge University Press, 1970, pp. 73–75, 137–139, 151–156.

6 Shames, I. H., *Mechanics of Fluids*, McGraw-Hill, 1962, pp. 77–155.

7 *IBM Continuous System Modeling Program III*, Program Reference Manual No. 5734-XS9.

8 El-Wakil, M. M., *Nuclear Heat Transport*, International, 1971, pp. 238–248.

9 Rohsenow, W. M., and Choi, H. Y., *Heat Mass and Momentum Transfer*, Prentice Hall, 1961, pp. 192–196.

10 Tong, L. S., *Boiling Heat Transfer and Two-Phase Flow*, Wiley, 1965, pp. 111–134.

APPENDIX

Summary of Equation Set Constituting the Mathematical Model

The following differential equations identify the selected state variables as l_{13}, u_2, l_{15}, u_6, ρ_5, T_{m2}, T_{m4}, T_{m6}, and h_1, respectively:

$$\frac{dl_{13}}{dt} = \left[W_1 - W_3 - \left(\frac{\partial \rho_2}{\partial u_2}\right)_{P2} (W_1 (h_1 - u_2) - W_3 (h_3 - u_2) + Q_2)/\rho_2 \right] \Big/ \left[A \left(\rho_2 - \rho_3 + (\rho_3/\rho_2) \left(\frac{\partial \rho_2}{\partial u_2}\right)_{P_2} (h_3 - u_2) \right) \right]$$

$$\frac{du_2}{dt} = [(W_1(h_1 - u_2) - W_3(h_3 - u_2) + Q_2)/A + \rho_3(h_3 - u_2)\, dl_{13}/dt]/(\rho_2\, l_{13})$$

$$\frac{dl_{15}}{dt} = [\rho_3(h_3 - u_4)\, dl_{13}/dt - (W_3(h_3 - u_4) - W_5 (h_5 - u_4) + Q_4)/A + \rho_4\, l_{35}\, du_4/dt]/(\rho_5 (h_5 - u_4))$$

$$\frac{du_6}{dt} = ((W_5 (h_5 - u_6) - W_7 (h_7 - u_6) + Q_6)/A - \rho_5 (h_5 - u_6)\, dl_{15}/dt)/(\rho_6 l_{57})$$

$$\frac{d\rho_5}{dt} = ((W_3 - W_7)/A + (\rho_5 - \rho_3)\, dl_{13}/dt)/(l_{35} + l_{57})$$

$$\frac{dT_{m2}}{dt} = (Q_{g2} - Q_2)/(C_m l_{13}) + ((T_{m4} - T_{m2})/l_{15})\, dl_{13}/dt$$

$$\frac{dT_{m4}}{dt} = (Q_{g4} - Q_4)/(C_m l_{35}) + ((T_{m6} - T_{m4})/(l_{35} + l_{57}))\, dl_{15}/dt + ((T_{m4} - T_{m2})/l_{15})\, dl_{13}/dt$$

$$\frac{dT_{m6}}{dt} = (Q_{g6} - Q_6)/(C_m l_{57}) + ((T_{m6} - T_{m4})/(l_{35} + l_{57}))\, dl_{15}/dt$$

$$\frac{dh_1}{dt} = (h_{fw} - h_1)/(A l_{13}\rho_2/(2W_1)) \text{ where } h_{fw} \text{ is feedwater enthalpy}$$

The supporting algebraic equations are given below:

$$P_1 = P_3 + K_{f2} W_1^2 l_{13}/\rho_2 + \rho_2 g l_{13} \sin\theta$$

$$W_3 = \sqrt{(P_3 - P_5 - \rho_4 g l_{35} \sin\theta)\, \rho_4/(K_{f4} l_{35})}$$

$$W_7 = \sqrt{(P_5 - P_7 - \rho_6 g l_{57} \sin\theta)\, \rho_6/(K_{f6} l_{57})}$$

$$W_5 = (W_3 + W_7)/2 \text{ and } l_{13} + l_{35} + l_{57} = l_{15} + l_{57} = l_{17} \text{ (a constant)}$$

$$Q_{g2} = A_0 l_{13} (T_{g2} - T_{m2})/(K_{gm2} G^{-0.66} + C_0)$$

where $C_0 = [r_0 ln (r_0/r_m)]/k_m$ and $r_m = (r_0 + r_i)/2$

$$Q_{g4} = A_0 l_{35} (T_{g4} - T_{m4})/(K_{gm4} G^{-0.66} + C_0)$$

$$Q_{g6} = A_0 l_{57} (T_{g6} - T_{m6})/(K_{gm6} G^{-0.66} + C_0)$$

$$Q_2 = A_i l_{13} (T_{m2} - T_2)/(K_{mf2} W_1^{-0.8} + C_i)$$

where $C_i = [r_i ln (r_m/r_i)]/k_m$

$$Q_4 = A_i l_{35} (T_{m4} - T_4)/(K_{mf4} + C_i)$$

$$Q_6 = A_i l_{57} (T_{m6} - T_6)/(K_{mf6} W_7^{-0.88} + C_i)$$

$$T_{g5} = (T_{g7} (1 - Y_6) + 2 Y_6 T_{m6} - Y_g\, dl_{15}/dt)/(1 + Y_6)$$

where $Y_6 = A_0 l_{57}/(2(K_{gm6} G^{-0.66} + C_0)\, G\, C_p)$,

$Y_g = (C_p - C_v)\, A_g K_{\rho T}/(G C_p)$ and $C_0 = (r_0 ln (r_0/r_m))/k_m$

$$T_{g3} = (T_{g5} (1 - Y_4) + 2 Y_4 T_{m4} + Y_g\, dl_{35}/dt)/(1 + Y_4)$$

where $Y_4 = A_0 l_{35}/(2(K_{gm4} G^{-0.66} + C_0)\, G\, C_p)$

$$T_{g1} = (T_{g3} (1 - Y_2 + 2 Y_2 T_{m2} + Y_g\, dl_{13}/dt)/(1 + Y_2)$$

where $Y_2 = A_0 l_{13}/(2(K_{gm2} G^{-0.66} + C_0)\, G\, C_p)$

$$T_{gi} = (T_{g(i-1)} + T_{g(i+1)})/2,\ i = 2, 4, 6$$

The following process variables were obtained by thermodynamic state relationship and/or averaging interpolation/extrapolation:

$h_5, P_5, T_5 = f(\rho_5)$

$P_6 = \text{Avi}\ (P_5, P_7)$

$\rho_6, h_6, T_6 = f(u_6, P_6)$

$h_7 = \text{Ave}\ (h_5, h_6)$

$T_7 = f(h_7, P_7)$

$h_2, \rho_2, T_2 = f(u_2)$

$h_3 = \text{Ave}\ (h_1, h_2)$

$P_3, \rho_3, T_3 = f(h_3)$

$T_4 = \text{Avi}\ (T_3, T_5)$

$\rho_4 = \text{Avi}\ (\rho_3, \rho_5)$

$h_4 = \text{Avi}\ (h_3, h_5)$

$u_4 = f(h_4, \rho_4)$

$$\frac{du_4}{dt} = \text{Avi}\left(\frac{du_2}{dt}, \left(\frac{\partial u}{\partial \rho}\right)_{x=1} \frac{d\rho_5}{dt}\right)$$

where $f(\ )$ indicates a function

Avi( ) indicates value obtained by averaging interpolation

Ave( ) indicates value obtained by averaging extrapolation

Printed in U.S.A.